

PREPARED FOR SUBMISSION TO JINST

INSTRUMENTATION OF COLLIDING BEAM PHYSICS, FEBRUARY 24-28, 2020, NOVOSIBIRSK, RUSSIA

## Scintillation properties of $(\text{Zn}_{0.9}\text{Pb}_{0.1})(\text{W}_{0.9}\text{Mo}_{0.1})\text{O}_4$ and $(\text{Zn}_{0.9}\text{Cd}_{0.1})(\text{W}_{0.9}\text{Mo}_{0.1})\text{O}_4$ mixed crystals

---

**E.N. Galashov,<sup>a</sup> D.V. Matvienko,<sup>a,b,1</sup> V.A. Moskovskiy,<sup>a</sup> B.I. Sikach<sup>b</sup> and B.A. Shwartz<sup>a,b</sup>**

<sup>a</sup>*Novosibirsk State University,  
630090, Pirogova st. 2, Novosibirsk, Russia*

<sup>b</sup>*Budker Institute of Nuclear Physics SB RAS,  
630090, Lavrentieva av., 11, Novosibirsk, Russia*

*E-mail:* [d.v.matvienko@inp.nsk.su](mailto:d.v.matvienko@inp.nsk.su)

**ABSTRACT:** Scintillation properties of  $(\text{Zn}_{0.9}\text{Pb}_{0.1})(\text{W}_{0.9}\text{Mo}_{0.1})\text{O}_4$  and  $(\text{Zn}_{0.9}\text{Cd}_{0.1})(\text{W}_{0.9}\text{Mo}_{0.1})\text{O}_4$  mixed crystals with doping of Eu, Sm, Pr, Ce, Sc, Yt and Nb are studied. Measurements of their light yields relative to pure  $\text{ZnWO}_4$  at room temperature, decay times and energy resolutions at 662 keV are presented. Emission spectra are obtained with  $^{239}\text{Pu}$  source of alpha particles.

**KEYWORDS:** Scintillators, scintillation and light emission processes (solid, gas and liquid scintillators); Interaction of radiation with matter

---

<sup>1</sup>Corresponding author

---

## Contents

<b>1</b>	<b>Introduction</b>	<b>1</b>
<b>2</b>	<b>Experimental details</b>	<b>2</b>
<b>3</b>	<b>Decay time</b>	<b>3</b>
<b>4</b>	<b>Light yield relative to pure ZnWO<sub>4</sub></b>	<b>4</b>
<b>5</b>	<b>Emission spectrum</b>	<b>6</b>
<b>6</b>	<b>Conclusion</b>	<b>7</b>

---

## 1 Introduction

A weak interacting massive particle (WIMP) is one of the proposed candidates for dark matter. Despite of the fact that most of the WIMP models are strongly constrained by direct, indirect and LHC searches, their parameter spaces are far from full exclusion. One of the direct search options are experiments with low temperature crystals, CRESST [1], EDELWEISS [2], CDMS [3] and proposed EURECA project [4]. The CRESST experiment operates with CaWO<sub>4</sub> crystals as absorbers. In these crystals a WIMP particle could be elastically scattered on nuclei producing low energy nuclear recoils. The interaction produces heat and a small fraction of energy deposited is emitted as scintillation light. Since the light pulse produced differs for the different types of particle interaction ( $\alpha/\beta$ -particles,  $\gamma$ -quanta, neutrons), a powerful background discrimination with remarkable energy threshold and resolution could be achieved. The last results provided by the CRESST collaboration [1] show sensitivity for WIMP-nucleus cross section down to  $10^{-6}$  pb. This value is a few orders of higher than one achieved by liquid-xenon experiments (LUX [5], XENON1T [6] and PandaX [7]). However cryogenic crystal experiments can be still competitive. The new EURECA project has been extensively discussed last years. It is a multi-target large experiment aimed to achieve a limit of spin-independent WIMP-nucleus cross section of  $10^{-10} - 10^{-11}$  pb. Such limit requires very low radioactive contamination of the materials used as well as high light yields at cryogenic temperatures. A family of heavy inorganic scintillators ABO<sub>4</sub> (A=Zn, Ca, Cd and B=Mo, W) is considered as an attractive target [8].

The other potential application of such crystals comes from experiments aimed to search for neutrinoless double beta decay ( $0\nu2\beta$ ). The great interest of such decay is explained by observed neutrino oscillations which prove nonzero neutrino masses. The  $0\nu2\beta$  decay can give a complementary information to neutrino oscillation experiments and establish the Majorana nature of neutrino ( $\nu = \bar{\nu}$ ). In addition, an effective neutrino mass extracting from the  $0\nu2\beta$  decay can constrain the sterile neutrino parameter space [9]. The AMoRE experiment [10] aims to search for

$0\nu2\beta$  decay of  $^{100}\text{Mo}$  nuclei using  $\text{CaMoO}_4$  scintillating crystals operating at cryogenic temperatures. The detection principle is similar to WIMP searches. The simultaneous measurement of light and phonon signals allows one to suppress a major alpha background occurring from radioactive contamination. The R&D studies consider various other molybdate crystals for the experiment upgrade to avoid high-expensive depleting of  $^{40}\text{Ca}$  isotopes, which produce an internal background.

A zinc tungstate ( $\text{ZnWO}_4$ ) scintillator is also discussed as a very promising material for WIMP and  $0\nu2\beta$  searches. An advantage of these crystals is that their light yield for heavy particles (nuclear recoils, alpha) varies according to the orientation of the particle path into the crystal with respect to the crystallographic axes. Such tendency is absent for  $e/\gamma$  radiation which is isotropic. In addition, the crystals show high radiopurity properties. It gives a possibility to search for diurnal modulation of WIMP direction with  $\text{ZnWO}_4$  crystals [11]. A natural abundance of  $^{64}\text{Zn}$  and  $^{186}\text{W}$  isotopes is relatively large. The  $2\nu2\beta$  decay of  $^{186}\text{W}$  is expected to be suppressed. It provides a suitable conditions to search for  $0\nu2\beta$  decays. The transition  $^{64}_{30}\text{Zn} \longrightarrow ^{64}_{28}\text{Ni}$  allows one to search for double electron capture and electron capture with positron emission.

The promising properties of  $\text{ZnWO}_4$  crystals provide a strong motivation to further improve performance of this material by growth of mixed and co-doped crystals based on  $\text{ZnWO}_4$  wolframite crystal structure and  $\text{CdMoO}_4$  (or  $\text{PbMoO}_4$ ) scheelite-type structure. In this study we consider the eight crystal compounds derived from  $\text{ZnWO}_4$  and  $\text{CdMoO}_4$  (or  $\text{PbMoO}_4$ ) solid solutions and mixed with 90% and 10% proportions. The obtained mixed structures are doped with (1 at. %) ion-activators. The molecular formula can be written as  $(\text{Zn}_{0.9}\text{Li}_{0.01}\text{X}_{0.1})(\text{W}_{0.9}\text{Mo}_{0.1})\text{O}_4$  (Y), where  $\text{Y} = \text{Eu, Sm, Pr}$  for  $\text{X} = \text{Pb}$  ( $\text{ZnWPbMoO}_4(\text{Y})$ ) and  $\text{Y} = \text{Eu, Ce, Sc, Yt, Nb}$  for  $\text{X} = \text{Cd}$  ( $\text{ZnWCdMoO}_4(\text{Y})$ ). In addition, one crystal without doping for  $\text{X} = \text{Cd}$  is used. Lithium ions are inserted to compensate a charge of ion-activators. The  $\text{ZnWPbMoO}_4(\text{Y})$  and  $\text{ZnWCdMoO}_4(\text{Y})$  single crystals were grown in air on platinum crucible of 40 mm in diameter according to the low-thermal-gradient Czochralski method in the Department of Applied Physics at Novosibirsk State University, Novosibirsk, Russia. The start growth temperature is  $1182^\circ\text{C}$  and  $1192^\circ\text{C}$ , which is lower than  $\text{ZnWO}_4$  ( $1202^\circ\text{C}$ ). The growth direction is  $[010]$ . During the crystal growth the crystal-melt interface was polyhedral, represented mainly by plane  $(010)$ . A pure  $\text{ZnWO}_4$  crystal grown by the same technique is used as a reference for our study.

A comparative analysis of scintillation properties for pure  $\text{ZnWO}_4$  and grown mixed samples is performed with the 662 keV photons from  $^{137}\text{Cs}$  source at room temperature. An emission spectrum is evaluated with  $^{239}\text{Pu}$  source of  $\alpha$ -particles.

## 2 Experimental details

The  $\text{ZnWCdMoO}_4(\text{Y})$  crystals have cubic shapes with the size of 12 mm while the  $\text{ZnWPbMoO}_4(\text{Y})$  crystals have quarter-cylinder shapes with the average cross section about  $200\text{ mm}^2$  and height 13 mm. The reference  $\text{ZnWO}_4$  crystal has a cylindrical shape with the diameter of 30 mm and height of 11 mm. All samples are wrapped in two layers of  $200\text{ }\mu\text{m}$  porous teflon coverage where the bottom face is kept to be opened.

The measurements of scintillation characteristics are carried out using experimental setup shown in figure 1. The crystal is positioned on the photomultiplier tube (PMT) Hamamtsu R1847S with optical grease BC-630. The PMT has a bialkali photocathode and borosilicate glass window,

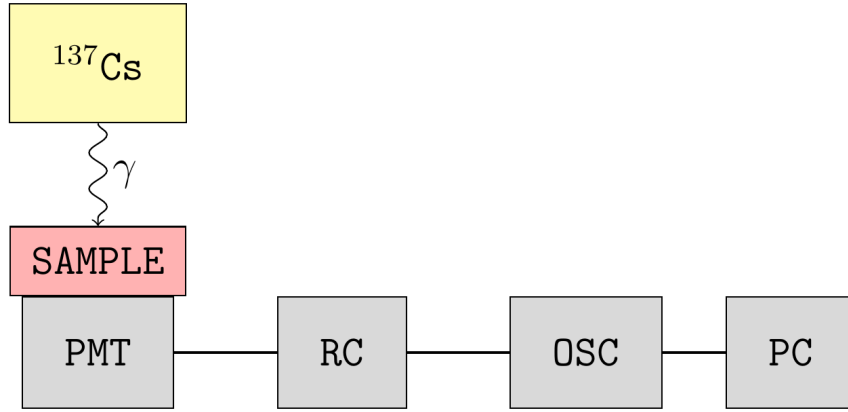


**Figure 1:** Principal scheme of experimental setup to measure the scintillation properties of the studied crystals.

linear focused ten-stage dynode system with a typical gain of the order of  $10^7$  and spectral response in the range from 300 nm to 650 nm with maximum quantum efficiency of 28% at 420 nm. The crystal is irradiated by a  $^{137}\text{Cs}$  source of 662 keV photons and resulting scintillation light is detected. The signal pulses are shaped by a RC-circuit with time constant of 750 nsec to decrease the rate of false triggers and recorded by oscilloscope OWON TDS8204 within 150  $\mu\text{s}$  time gate. Pulse shape analysis includes calculation of baseline, determination of signal arrival, pulse height and integrated signal within tuned time window.

The PMT is calibrated by a single photoelectron method. An external light source CAEN LED driver SP5601 generating ultra-fast monochromatic pulses is used. The light intensity is adjusted in such a way that only one or several photoelectrons are emitted from the PMT photocathode.

### 3 Decay time

Decay time characteristics of the scintillation pulse of the studied crystals are obtained by the fit of the average pulse shape measured by oscilloscope when the crystal is irradiated by 662 keV  $\gamma$ -quanta. The average pulse is built from individual pulses falling into the full absorption peak of the crystal energy spectrum. The pulse shape is fitted by two decay exponential functions with the lifetimes of the fast and slow components and one exponential function describing the rise of the pulse. The functions are corrected to the non-zero integration constant of electronics (750 nsec). The average pulse and result of the fit for the reference  $\text{ZnWO}_4$  crystal are shown in figure 2. The decay components and these intensities are in reasonable agreement with those obtained in ref. [13] (see table 1). Our measurement is not sensitive to the fast component of 0.7  $\mu\text{sec}$  in ref. [13] due to limited timing resolution in the pulse shape. The decay time constants of the  $\text{ZnWPbMoO}_4$  and  $\text{ZnWCdMoO}_4$  samples measured with the same method as for the pure  $\text{ZnWO}_4$  crystal are presented in table 2. All the crystals show decay characteristics (at least, for 662 keV photons) close to the values obtained for the reference  $\text{ZnWO}_4$  crystal. Although, some tendency against higher decay

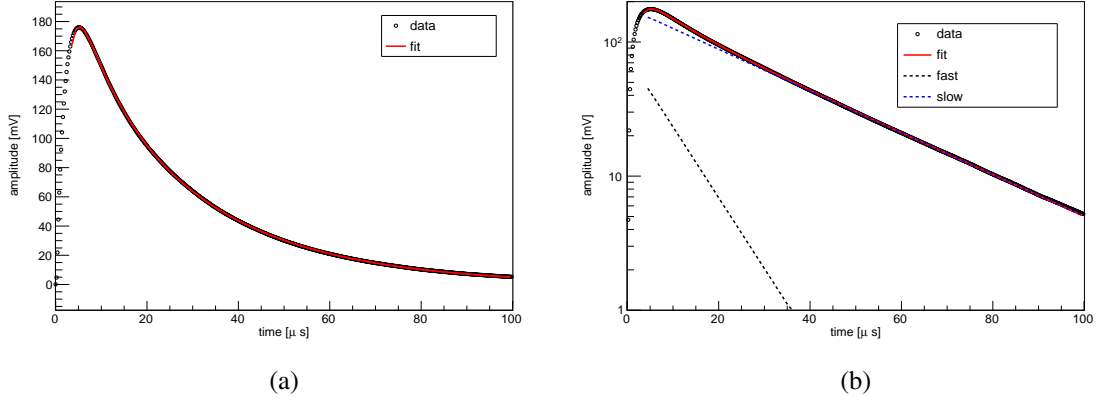


**Figure 2:** Average pulse shape for the pure  $\text{ZnWO}_4$  crystal shown in (a) linear scale and (b) log scale. The red line shows the fit result, which gives  $8.2 \mu\text{sec}$  for the fast component (black dashed line) and  $27.9 \mu\text{sec}$  for the slow one (blue dashed line). Intensities of the components are 11% and 89%, respectively.

**Table 1:** Decay times and their intensities of  $\text{ZnWO}_4$  scintillator for 662 keV  $\gamma$ -quanta. The results are compared to those in ref. [13].

Decay components	This work	Ref. [13]
Fast, $\mu\text{sec}$ (%)	—	0.7 (2)
Fast, $\mu\text{sec}$ (%)	8.2 (11)	7.5 (9)
Slow, $\mu\text{sec}$ (%)	27.9 (89)	25.9 (89)

**Table 2:** Decay times and their relative intensities (shown in percentage of the total intensity) of the  $\text{ZnWPbMoO}_4$  and  $\text{ZnWCdMoO}_4$  samples. The result for the reference  $\text{ZnWO}_4$  is also shown.

Sample	Fast		Slow		Sample	Fast		Slow	
	$\mu\text{sec}$	%	$\mu\text{sec}$	%		$\mu\text{sec}$	%	$\mu\text{sec}$	%
$\text{ZnWO}_4$	8.2	11	27.9	89	$\text{ZnWCdMoO}_4(\text{Eu})$	9.3	15	28.5	85
$\text{ZnWPbMoO}_4(\text{Eu})$	12.5	24	32.0	76	$\text{ZnWCdMoO}_4(\text{Ce})$	8.5	13	28.3	87
$\text{ZnWPbMoO}_4(\text{Sm})$	12.6	23	32.0	77	$\text{ZnWCdMoO}_4(\text{Sc})$	8.7	14	28.3	86
$\text{ZnWPbMoO}_4(\text{Pr})$	13.1	26	32.5	74	$\text{ZnWCdMoO}_4(\text{Yt})$	8.4	11	28.1	89
$\text{ZnWCdMoO}_4$	10.9	15	29.3	85	$\text{ZnWCdMoO}_4(\text{Nb})$	11.3	16	29.0	84

time values and intensities for the fast components is observed for the  $\text{ZnWCdMoO}_4$  crystals and, especially, for the  $\text{ZnWPbMoO}_4$  sample. All measurements are performed at room temperature.

#### 4 Light yield relative to pure $\text{ZnWO}_4$

The light yield of the scintillation counter is its important characteristic. In this study the light yield of all crystals is measured relative to the pure  $\text{ZnWO}_4$  sample. Our setup with the calibrated PMT allows us to measure the number of photoelectrons corresponding to the full absorption of 662 keV

photons inside the crystal. The signal shape is integrated within 30  $\mu\text{sec}$  and integral spectrum in terms of number of photoelectrons is obtained.  $^{137}\text{Cs}$  energy spectra of the pure  $\text{ZnWO}_4$  sample and  $\text{ZnWCdMoO}_4(\text{Yt})$  crystal with the highest photoelectron yield among other samples are shown in figure 3. Total absorption peaks are clearly seen and fitted by the Gaussian function to extract

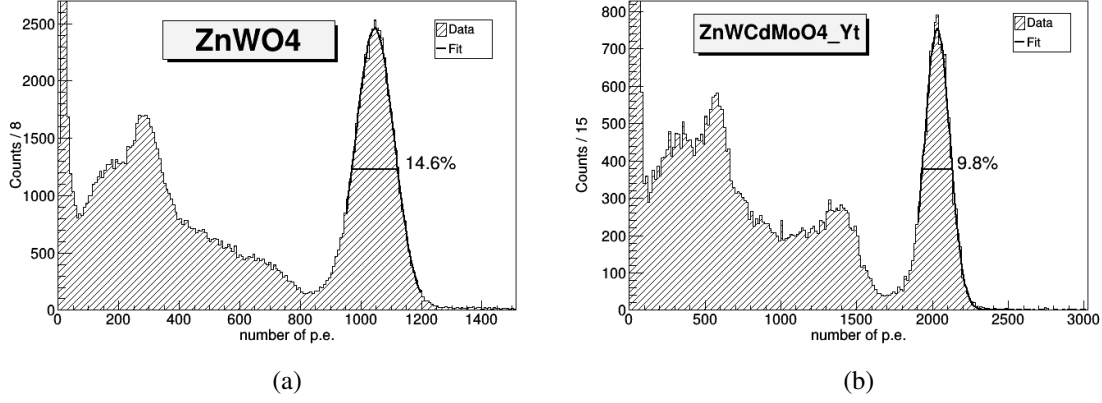


**Figure 3:**  $^{137}\text{Cs}$  energy spectra measured with (a)  $\text{ZnWO}$  and (b)  $\text{ZnCdWO}(\text{Yt})$  crystals. The full absorption peak is fitted to the Gaussian function.

the photoelectron yield. The relative energy resolution of 14.6% for the  $\text{ZnWO}_4$  and 9.8% for the  $\text{ZnWCdMoO}_4(\text{Yt})$  is calculated as a full width at half maximum (FWHM) of the photopeak divided by the number of photoelectrons. The total resolution includes the scintillator resolution and the statistical contribution related to the variation of the number of photoelectrons produced at the photocathode.

The spectra for all studied samples are similar to that of the  $\text{ZnWCdMoO}_4(\text{Yt})$ . Their characteristics are shown in table 3.

**Table 3:** Light yield characteristics and scintillator resolutions of the  $\text{ZnWPbMoO}_4$  and  $\text{ZnWCdMoO}_4$  samples. The result for the reference  $\text{ZnWO}_4$  is also shown.

Crystal	$N_{p.e}/\text{MeV}$	Relative light yield	Scintillator resol, %
$\text{ZnWO}_4$	1580	1.0	12.2
$\text{ZnWPbMoO}_4(\text{Eu})$	2705	1.7	8.1
$\text{ZnWPbMoO}_4(\text{Sm})$	2535	1.6	8.5
$\text{ZnWPbMoO}_4(\text{Pr})$	2491	1.6	10.6
$\text{ZnWCdMoO}_4$	2799	1.8	7.9
$\text{ZnWCdMoO}_4(\text{Eu})$	3012	1.9	9.3
$\text{ZnWCdMoO}_4(\text{Ce})$	2971	1.9	9.2
$\text{ZnWCdMoO}_4(\text{Sc})$	2992	1.9	9.3
$\text{ZnWCdMoO}_4(\text{Yt})$	3066	1.9	7.9
$\text{ZnWCdMoO}_4(\text{Nb})$	2932	1.9	7.8

Light yields are defined relative to the light yield of the reference  $\text{ZnWO}_4$  crystal. In the first approximation, the spectral sensitivities of the studied samples are considered to be identical with the  $\text{ZnWO}_4$  as it is shown in section 5. Light collection efficiencies of the studied samples are estimated at the level of 50 – 60% based on the ratio of values measured with and without optical grease. In such a way, a ratio of light yields is estimated as a ratio of photoelectron yields (see table 3).

The light yields of the new mixed crystals are enhanced relative to the  $\text{ZnWO}_4$  by a factor of 1.5 for the  $\text{ZnWPbMoO}_4$  crystals and two for the  $\text{ZnWCdMoO}_4$ . Their energy resolutions are also significantly improved from 12.2% for the reference  $\text{ZnWO}_4$  to 7.8% for the  $\text{ZnWCdMoO}_4(\text{Nb})$ . All these measurements are performed at room temperature with a  $^{137}\text{Cs}$  source of 662 keV photons.

## 5 Emission spectrum

Emission spectrum of the studied crystals is estimated using a set of five color glass cut-on filters Newport FS-C, which are placed on the window of the PMT. The scintillator is put on the filter and irradiated by a  $^{239}\text{Pu}$  source of  $\alpha$  particles with the energy of 5156 keV that provides a single peak clearly distinguished even for low light signal. To avoid the  $\alpha$  particle absorption in the teflon coverage, the small hole about  $1 \text{ mm}^2$  is made in the centre of the top face.

The relative light yield with each filter  $F_i$  is measured as  $L_i = A_i/A_0$ , where  $A_i$  and  $A_0$  are energy spectrum peak positions with and without filter  $F_i$ , respectively. Then, the relative light yield  $s_{ij}$  in the wavelength range  $[\lambda_i, \lambda_j]$  ( $j = i + 1$ ) is given by

$$s_{ij} = (L_i/R_i - L_j/R_j) / \int_{\lambda_i}^{\lambda_j} Q(\lambda) d\lambda, \quad (5.1)$$

where  $R_i$  is a transmission coefficient of the filter  $F_i$  at  $\lambda > \lambda_i$  and  $Q(\lambda)$  is the PMT quantum efficiency.

The resulting emission spectra are shown in figure 4. The emission spectrum of pure  $\text{ZnWO}_4$

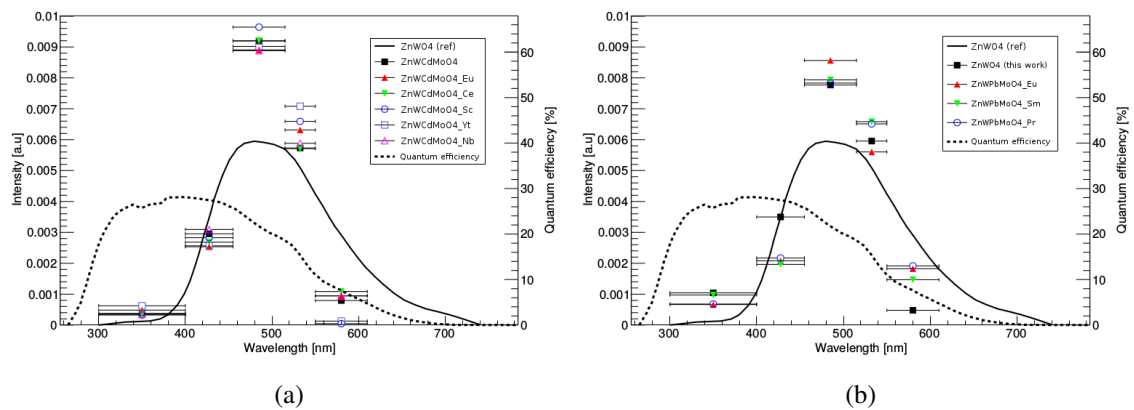


**Figure 4:** Emission spectra of (a)  $\text{ZnWCdMoO}_4$  and (b)  $\text{ZnWPbMoO}_4$  samples. The spectrum of the reference  $\text{ZnWO}_4$  crystal is also measured. The solid line shows the known emission spectrum of  $\text{ZnWO}_4$  taken from ref. [12]. The dashed line corresponds to the PMT quantum efficiency curve.

crystal is taken from ref. [12]. We can see that all spectra peak at value lying in the range between 460 nm and 520 nm where the maximum intensity of the pure  $\text{ZnWO}_4$  (480 nm) is achieved. The PMT quantum efficiency is superimposed on the plot.

## 6 Conclusion

Tungstate and molybdate crystals are considered as promising materials for cryogenic experiments hunting on WIMP particles or  $0\nu 2\beta$  decays. Several new  $(\text{Zn}_{0.9}\text{Pb}_{0.1})(\text{W}_{0.9}\text{Mo}_{0.1})\text{O}_4$  and  $(\text{Zn}_{0.9}\text{Cd}_{0.1})(\text{W}_{0.9}\text{Mo}_{0.1})\text{O}_4$  mixed crystals doped with of Eu, Sm, Pr, Ce, Sc, Yt and Nb and produced using low-thermal-gradient Czochralski process are studied. Their scintillation characteristics are measured at room temperature. Light yields, energy resolutions and scintillation decay times are obtained with  $^{137}\text{Cs}$  source of gamma quanta while spectral sensitivities are evaluated with  $^{239}\text{Pu}$  source of alpha particles.

Analysis of emission spectra and decay time components shows the properties similar to the pure  $\text{ZnWO}_4$  crystal. However, the light yields of the samples are increased by a factor of up to two relative to the reference  $\text{ZnWO}_4$  scintillator (with the light yield of about 10 ph./keV), especially for  $(\text{Zn}_{0.9}\text{Cd}_{0.1})(\text{W}_{0.9}\text{Mo}_{0.1})\text{O}_4$  samples. Their energy resolutions are also significantly improved up to 7.8%. Other studies of their performance are required at low temperatures to understand a benefit of their potential application in cryogenic experiments.

## Acknowledgments

The work of E.N.G and V.A.M is supported by the Ministry of Education and Science of the Russian Federation (grant No. 3.3726.2017). The work of D.V.M is supported by the Russian Federation Government (grant No. 14.W03.31.0026).

## References

- [1] M. Mancuso *et al.* [CRESST Collaboration], “Searches for Light Dark Matter with the CRESST-III Experiment,” *J. Low. Temp. Phys.* **199** (2020) no.1-2, 547.
- [2] E. Armengaud *et al.* [EDELWEISS Collaboration], “Searching for low-mass dark matter particles with a massive Ge bolometer operated above-ground,” *Phys. Rev. D* **99** (2019) 082003. [arXiv:1901.03588 [astro-ph.GA]]
- [3] R. Agnese *et al.* [SuperCDMS Collaboration], “Search for Low-Mass Dark Matter with CDMSlite Using a Profile Likelihood Fit,” *Phys. Rev. D* **99** (2019) 062001. [arXiv:1808.09098 [astro-ph.CO]].
- [4] G. Angloher *et al.* [EURECA Collaboration], “EURECA Conceptual Design Report,” *Phys. Dark Univ.* **3** (2014) 41.
- [5] D. S. Akerib *et al.* [LUX Collaboration], “Results of a Search for Sub-GeV Dark Matter Using 2013 LUX Data,” *Phys. Rev. Lett.* **122** (2019) no.13, 131301 [arXiv:1811.11241 [astro-ph.CO]].
- [6] E. Aprile *et al.* [XENON Collaboration], “Dark Matter Search Results from a One Ton-Year Exposure of XENON1T,” *Phys. Rev. Lett.* **121** (2018) no.11, 111302 [arXiv:1805.12562 [astro-ph.CO]].
- [7] C. Fu *et al.* [PandaX-II Collaboration], “Spin-Dependent Weakly-Interacting-Massive-Particle–Nucleon Cross Section Limits from First Data of PandaX-II



- Experiment*,” *Phys. Rev. Lett.* **118** (2017) no.7, 071301. Erratum: [*Phys. Rev. Lett.* **120** (2018) no.4, 049902] [arXiv:1611.06553 [hep-ex]].
- [8] L. L. Nagornaya *et al.*, “*Tungstate and molybdate scintillators to search for dark matter and double beta decay*,” *IEEE Trans. Nucl. Sci.* **56** (2009) 2513.
  - [9] A. Abada, A. Hernández-Cabezudo and X. Marciano, “*Beta and Neutrinoless Double Beta Decays with KeV Sterile Fermions*,” *JHEP* **1901** (2019) 041. [arXiv:1807.01331 [hep-ph]].
  - [10] V. Alenkov *et al.*, “*First Results from the AMoRE-Pilot neutrinoless double beta decay experiment*,” *Eur. Phys. J. C* **79** (2019) no.9, 791 [arXiv:1903.09483 [hep-ex]].
  - [11] F. Cappella *et al.*, “*On the potentiality of the  $\text{ZnWO}_4$  anisotropic detectors to measure the directionality of Dark Matter*,” *Eur. Phys. J. C* **73** (2013) no.1, 2276.
  - [12] H. Kraus, V. B. Mikhailik, Y. A. Ramachers, D. Day, K. B. Hutton and J. Telfer, “*Feasibility study of a  $\text{ZnWO}_4$  scintillator for exploiting materials signature in cryogenic WIMP dark matter searches*,” *Phys. Lett. B* **610** (2005) 37.
  - [13] F. A. Danevich, V. V. Kobychiev, S. S. Nagorny, D. V. Poda, V. I. Tretyak, S. S. Yurchenko and Y. G. Zdesenko, “ *$\text{ZnWO}_4$  crystals as detectors for  $2\beta$  decay and dark matter experiments*,” *Nucl. Instrum. Meth. A* **544** (2005) 553.